

Current Biology, Volume 29

Supplemental Information

Thalamic Drive of Cortical

Parvalbumin-Positive Interneurons

during Down States in Anesthetized Mice

Stefano Zucca, Valentina Pasquale, Pedro Lagomarsino de Leon Roig, Stefano Panzeri, and Tommaso Fellin

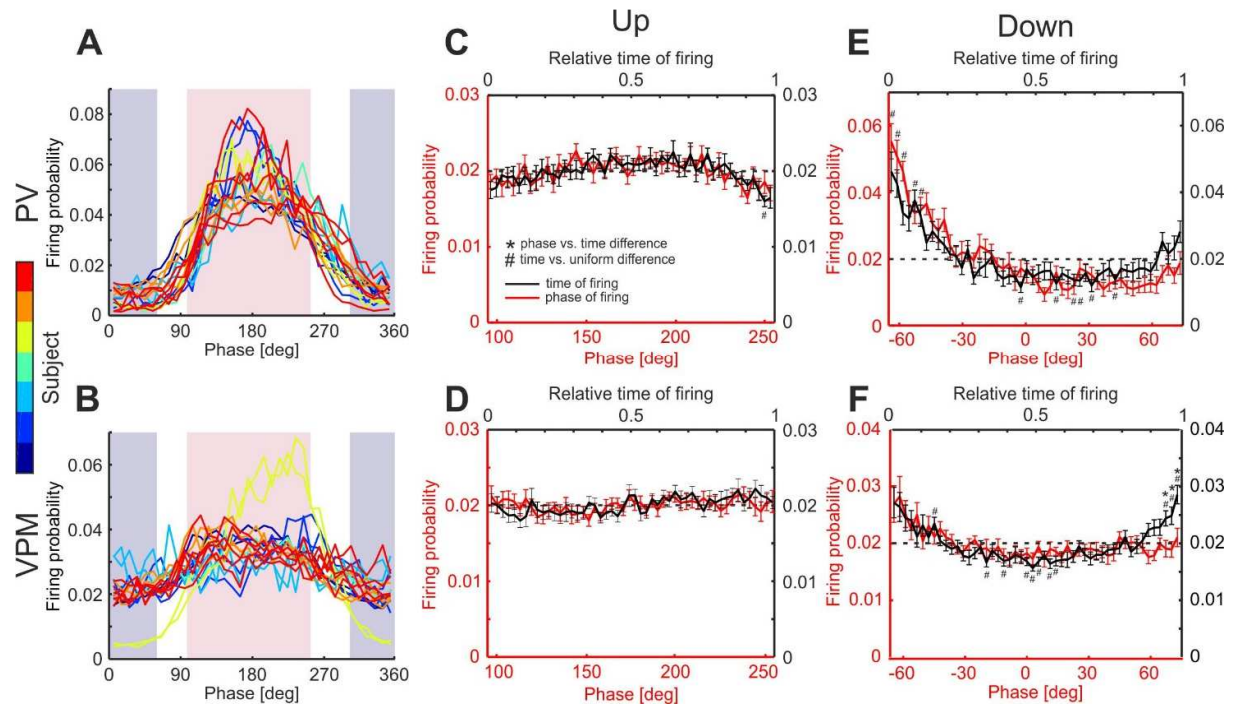
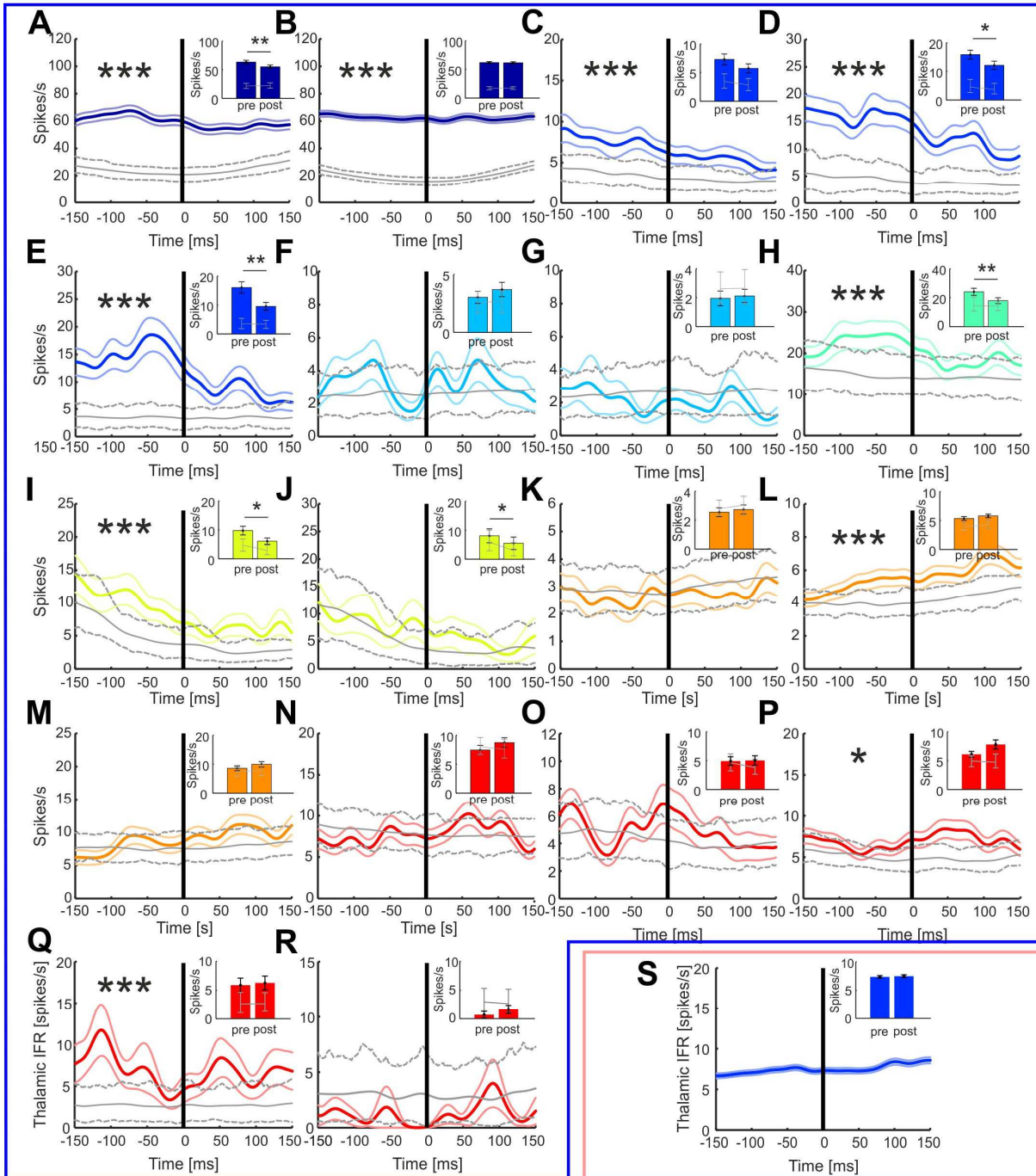


Figure S1. Phase-of-firing and relative time-of-firing distributions of PV cells and VPM MUA during cortical up- and down-states. Related to Figure 1. (A-B) Phase-of-firing distributions of all PV interneurons (color-coded by animal (A) and simultaneously recorded VPM MUA (B). **(C-D)** Phase-of-firing distribution (red, mean \pm s.e.m., $n = 18$ cells in 7 animals) and relative time-of-firing distribution (black) for PV interneurons (C) and VPM MUA (D) during cortical up-states. **(E-F)** Same as for (C, D), but for cortical down-states (mean \pm s.e.m., $n = 18$ recordings in 7 animals). For all panels: asterisks indicate point-wise significant statistical differences between the two curves (paired Student's t-test, FDR corrected for multiple comparisons, p -level = 0.05). Hashtags indicate point-wise significant statistical differences between time-of-firing distributions and the uniform distribution (one-sample Student's t-test, FDR corrected for multiple comparisons, p -level = 0.05).

Down-state



Up-state

Figure S2. Spike-triggered average analysis across individual experiments. Related to Figure 2. (A-R) Spike-triggered VPM firing rate based on PV interneuron spike times during cortical down-states for all recorded cells (n = 18 from 7 animals, Gaussian kernel standard deviation 12.5 ms, mean \pm s.e.m.). Statistical difference of the pre-spike VPM mean firing rate with respect to surrogate data is indicated by the asterisks (z-test, $p < 0.05$). Insets: VPM firing rate before and after a PV spike in down-state (pre: [-100, 0] ms; post: [0, 100] ms; mean \pm s.e.m.; Wilcoxon signed rank test). (S) Same as in (A-R) but for PV interneuron spike times during cortical up-states for one representative recorded cell.

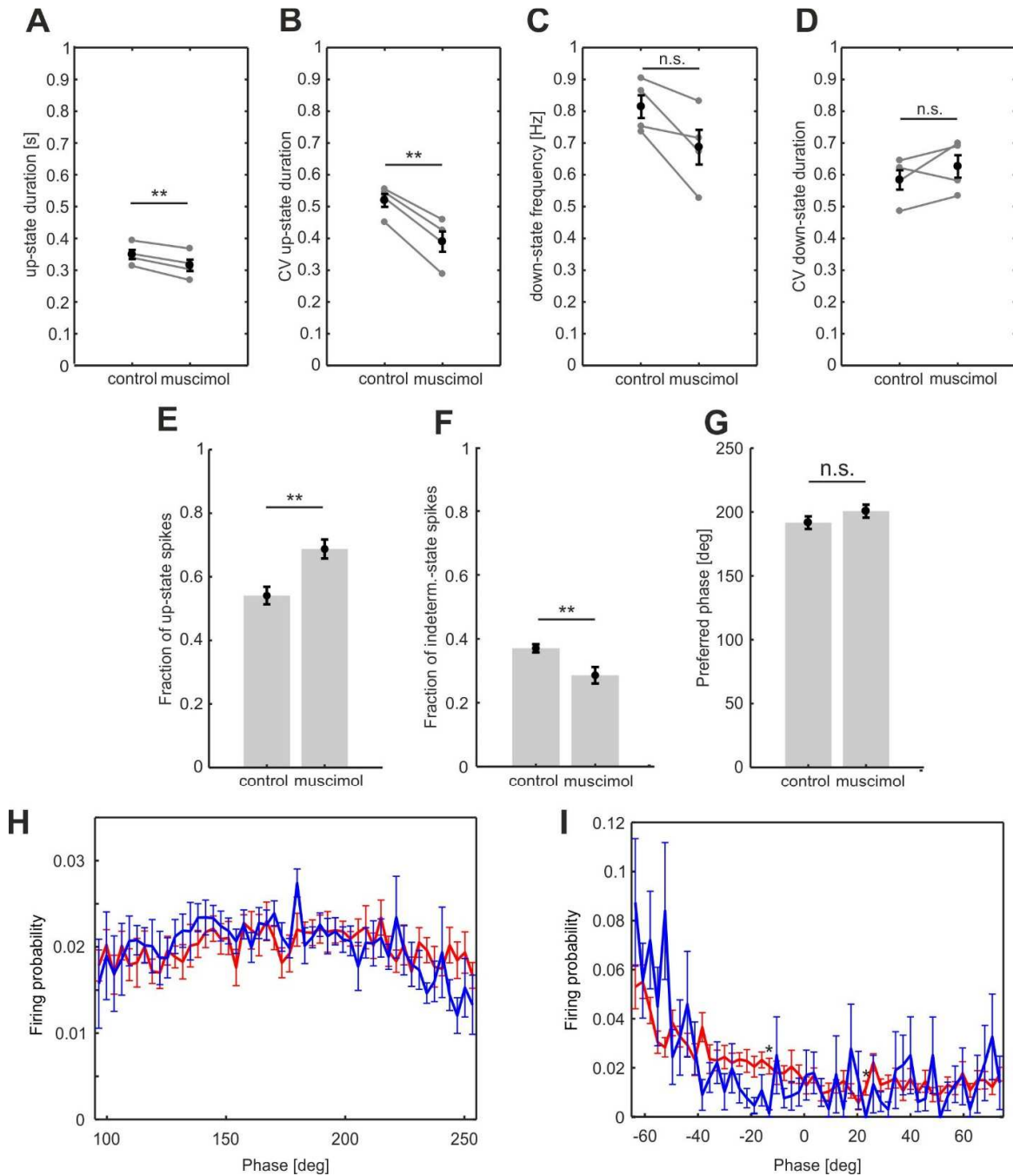


Figure S3. Effect of thalamic muscimol injection on cortical up and down-state dynamics and PV interneuron firing activity. Related to Figure 3. (A-B) Up-state duration (A) and its coefficient of variation (B) under control conditions and after muscimol injection in the thalamus (mean \pm s.e.m., paired Student's t-test, $p = 0.009$ for A and $p = 0.003$ for B, $n = 4$ animals). (C) Down-state frequency under control conditions and after muscimol injection in the thalamus (mean \pm s.e.m., paired Student's t-test, $n = 4$ animals). (D) Coefficient of variation of down-state duration under control conditions and after muscimol injection in the thalamus (mean \pm s.e.m., paired Student's t-test $p = 0.27$ for D, $n = 4$ animals). (E-F) Fraction of up (E) and indeterminate (F) state spikes under control conditions and after muscimol injection (mean \pm s.e.m., Student's t-test, $p = 0.003$ for C and $p = 0.008$ for D, control: $n = 8$ cells, muscimol: $n = 7$ cells from 4 animals). (G) Mean phase of firing of PV interneurons under control conditions and after thalamic muscimol injection (circular mean \pm s.e.m., $p = 0.26$, Watson-Williams test, control: $n = 8$, muscimol: $n = 7$ from 4 animals). (H-I) Phase-of-firing distribution of PV interneurons during cortical up (H) and down (I) states under control conditions (red, mean \pm s.e.m., $n = 8$ cells in 4 animals) and after thalamic muscimol injection (blue, mean \pm s.e.m., $n = 7$ cells in 4 animals). In both panels, the two curves do not show significant point-wise differences, except for two points (marked by asterisks, Student's t-test, FDR corrected for multiple comparisons, p -level = 0.05).

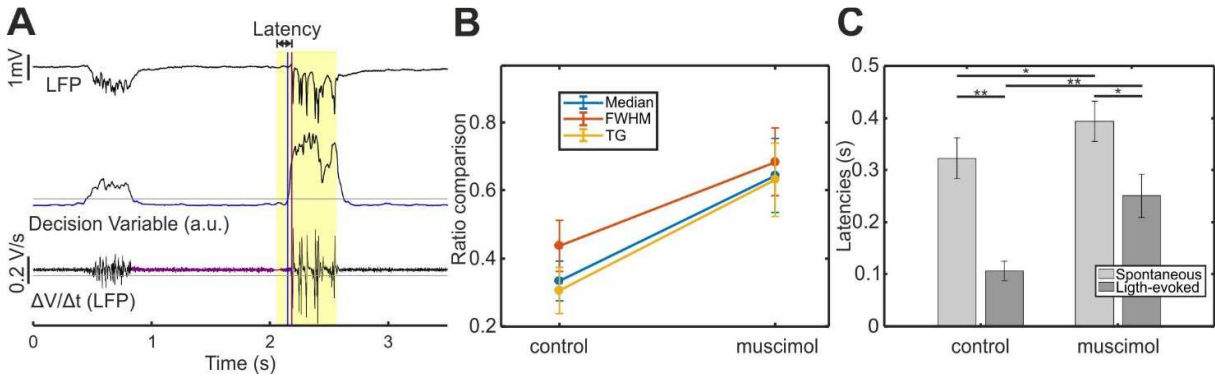


Figure S4. Latencies of down-to-up transitions upon inhibition of cortical PV interneurons under control condition and after thalamic pharmacological inactivation. Related to Figure 4. (A) Representative cortical LFP trace after muscimol injection in the thalamus (top) showing characteristic silent and active periods during slow oscillation network dynamics. The gamma-filtered signal (middle) is used to detect down-states (blue periods). This detection is then used to select the traces in which the beginning of the optogenetic inhibition of PV cells (yellow bar) occurred in a down-state. The transition to an up-state (purple vertical line) is defined as occurring when the LFP temporal derivative (bottom) crosses the threshold T (gray line). The latency of the transition is therefore the time interval between the beginning of the yellow bar and the purple vertical line. (B) Comparison of the average latency ratios calculated using three different thresholds (median, full-width-half-maximum and two-Gaussian mixture fitting, indicated by different colors) for down-state detection (see STAR Methods) (mean \pm s.e.m., one-way ANOVA, $p = 0.36$ for control and $p = 0.94$ for muscimol, $n = 7$ animals). (C) Latencies of spontaneous and light-evoked down-to-up transitions under control conditions and after muscimol application in the thalamus (mean \pm s.e.m., $n = 7$ animals).